Nonlinear contrast enhancement in photoacoustic molecular imaging with gold nanosphere encapsulated nanoemulsions

Chen-wei Wei,[1] Michael Lombardo,[1] Kjersta Larson-Smith,[1] Ivan Pelivanov,[1,2] Camilo Perez,[1] Jinjun Xia,[1] Thomas Matula,[1] Danilo Pozzo,[1] and Matthew O'Donnell[1]
[1]*Departments of Bioengineering and Chemical Engineering, and Applied Physics Lab, University of Washington, Seattle, Washington 98195, USA*
[2]*International Laser Center, Moscow State University, Moscow, Russian Federation*

(Received 6 December 2013; accepted 5 January 2014; published online 21 January 2014)

A composite contrast agent, a nanoemulsion bead with assembled gold nanospheres at the interface, is proposed to improve the specific contrast of photoacoustic molecular imaging. A phase transition in the bead's core is induced by absorption of a nanosecond laser pulse with a fairly low laser fluence (~3.5 mJ/cm^2), creating a transient microbubble through dramatically enhanced thermal expansion. This generates nonlinear photoacoustic signals with more than 10 times larger amplitude compared to that of a linear agent with the same optical absorption. By applying a differential scheme similar to ultrasound pulse inversion, more than 40 dB contrast enhancement is demonstrated with suppression of background signals. © *2014 AIP Publishing LLC*.
[http://dx.doi.org/10.1063/1.4862461]

Molecular imaging refers to sensing specific molecular pathways *in vivo* using non-invasive imaging techniques. In general, a specific, site-targeted exogenous agent (i.e., a nanoprobe) able to biochemically link to a selected biomarker is required, since the target molecules themselves are too small for non-invasive imaging. Photoacoustics (PA) is an attractive modality for molecular imaging, given its sub-mm spatial resolution, optical contrast, and multi-centimeter penetration depth.[1–3] In recent years, optically absorptive contrast agents, such as nanoparticles or particles with absorbing dye, have been widely used as targeted nanoprobes in many studies to improve the contrast of PA molecular imaging.[4–6] In most of these studies, contrast enhancement is proportional to contrast agent concentration and also depends on the incremental optical absorption of the agent compared to the background. In a heterogeneous environment with highly optically absorptive endogenous molecules, such as hemoglobin in the blood,[7] contrast specificity of the agent can be seriously degraded, especially for early stages of disease where aberrant cell number is very small or for rare cell types.[8]

In this study, a type of contrast agent with nonlinear response to applied laser fluence is investigated. It can enhance both the *sensitivity* of PA molecular imaging though efficient conversion of light energy to sound and the *specificity* of PA molecular imaging by suppressing any background signals linearly proportional to laser fluence. A diagram illustrating the structure of this contrast agent and the mechanism of generating a nonlinear PA signal is shown in Fig. 1. A nanoemulsion bead in water dispersion with absorbing particles assembled at the core-water interface, in particular, a perfluorohexane core with gold nanospheres (GNSs), is used in this study.[9] Due to clustering of GNSs, the absorption spectrum broadens to the near-infrared region (700–1000 nm) compared to the typical 520 nm absorption peak of distributed GNSs, enabling its use at depth in tissue for biomedical applications.

Under pulsed laser irradiation above a certain fluence threshold, heat flux released in the GNSs propagates into the bead's core, causing a phase-transition of perfluorohexane to form a microbubble. Consequently, much stronger PA signals are generated due to dramatically enhanced thermal expansion.[10] This phenomenon can be used to improve the sensitivity of PA molecular imaging and, more importantly, to greatly improve detection specificity. A similar idea has been recently published with a nanometer-scale droplet containing a perfluoropentane core and encapsulated gold nanorods, which can be optically triggered to form a gas bubble generating enhanced PA signals at a fixed laser fluence.[11]

In the current study, we found that generation of the acoustic signals from the beads' expansion behaves highly nonlinear, in terms of the relation of the signal amplitude versus applied laser fluence. An alternative contrast mechanism based on this fluence-dependent non-linearity is proposed here to distinguish nonlinear targeted objects from the linear background and, hence, enhance contrast specificity. Nonlinear contrast PA enhancement versus laser fluence was

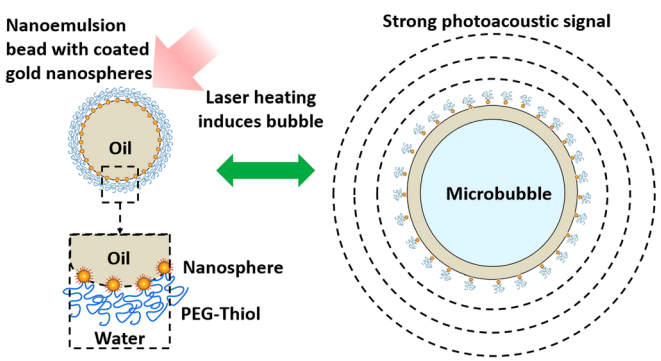

FIG. 1. Diagram of a nanoemulsion bead with a perfluorohexane core and gold nanospheres encapsulated on the oil-water interface, and laser pulse induced bubble formation of the bead. Heat released from the gold nanospheres induces a phase transition in the core, generating stronger photoacoustic signals compared to those by typical laser-sound conversion mechanism (i.e., thermal expansion).

studied in a recently published paper,[12] in which gold-coated carbon nanotubes in water were overheated by a pulsed laser to produce bubbles with subsequent nonlinear PA signal generation. However, the temperature threshold of bubble formation is 100 °C (i.e., boiling point of water), which may cause harm to surrounding normal live cells, and thus limit this approach for non-invasive *in vivo* imaging. In our approach, overheating occurs in the perfluorohexane core (boiling temperature = 56 °C) at temperatures much lower than 100 °C.

To demonstrate the nonlinear PA response of nanoemulsion beads with GNSs (NEB-GNSs), a series of PA images were recorded in a phantom at different laser fluences. The relationship between PA signal amplitude and applied laser fluence was investigated for NEB-GNSs, and the results were compared with a linear control agent (black ink of the same optical absorption coefficient) mimicking background absorbers. A scale-differential scheme was also applied to demonstrate enhanced specificity by removing linear background signals.

NEB-GNSs were produced using the same procedure described in the previous publications.[9,13] Colloidal GNSs with a mean diameter of 12 nm in an aqueous buffer were synthesized using a citrate reduction method.[14] The particles were functionalized using PEG-thiol and butane-thiol (Sigma Aldrich, St. Louis, MO, USA), with dosages of 4.0 chains/nm^2 Au and 500 molecules/nm^2 Au, respectively,[13] resulting in clustered GNS dispersions due to the attractive forces between the hydrophobic butane-thiol ligands.

A two-step sonication process was used to generate the emulsion beads using a digital sonifier with a microtip (102C, Branson, Danbury, CT, USA). A stock 5 vol. % perfluorohexane (Sigma Aldrich, St. Louis, MO, USA) in water emulsion was generated by pulsed sonication 1 s on, 4 s off, for a total of 2.5 min. The stock emulsion was then added into the clustered GNS dispersion and sonicated a second time. The final emulsion concentrations were 0.015 vol. % Au and 0.4 vol. % perfluorohexane in water, and the size was measured as 250 nm using dynamic light scattering. A monolayer of clustered GNSs adsorbed at the oil-water interface resulted in a broader and red-shifted absorption band (700–1000 nm).[9]

The non-linearity of NEB-GNSs was studied using a tube phantom (SLTT-16-72, Zeus, Orangeburg, SC, USA) with an energy-sweeping PA imaging system. A 532-nm pumped wavelength tunable optical parametric oscillator (OPO) laser (Surelite OPO plus, Continuum, Santa Clara, CA, USA) delivered 800-nm laser pulses, with a 10-ns duration at a 20-Hz repetition rate, to generate PA signals and also induce microbubbles by heating the NEB-GNSs. Before being coupled into a fiber bundle (77526, Oriel Instruments, Stratford, CT, USA), laser pulses passed through a continuously variable neutral density filter (NDL-10C-2, Thorlabs, Newton, NJ, USA) mounted on a linear actuator motor (T-LA60A, Zaber, Vancouver, BC, Canada) moving laterally to change the energy into the fiber bundle, producing a laser fluence varying from 2.3 mJ/cm^2 to 16.7 mJ/cm^2 on the sample in the tube immersed in a water tank. An ultrasound linear array transducer (AT8L12-5 50 mm, Broadsound, Hsinchu, Taiwan) interfaced with an ultrasound imaging system (Verasonics, Redmond, WA, USA) was placed about 15 mm above the tube to receive PA signals. The central 128 elements of the transducer were used, yielding a 25.6 mm aperture with a detection angle of about 81°. For comparison, a linear ink (Waterman, Paris, France) solution was used as a control. The absorption coefficient was adjusted to be the same, 2.5 cm^{-1}, for NEB-GNSs and ink at the irradiating wavelength.

PA images (cross-sectional view) of the two samples in the tube at three different laser fluences are shown in Fig. 2. Ink images (top row, (a)-(c)) depict typical PA images of a homogeneous cylindrical absorber detected by a band-limited ultrasound transducer. Only top and bottom boundaries can be seen, but not the middle part. The signal amplitude changes linearly with the applied laser fluence. In contrast, images of NEB-GNSs (bottom row, (d)-(f)) exhibit rapid signal growth as laser fluence increases due to nonlinear signal generation from bubble formation. Furthermore, the appearance of heterogeneous PA sources in the middle of the tube, especially at a laser fluence of 15 mJ/cm^2, is additional evidence of laser-induced transient bubble formation. Note that the display level for ink (maximum at −25 dB) and NEB-GNSs (maximum at 0 dB) is different to illustrate the amplitude difference between the two samples, and the

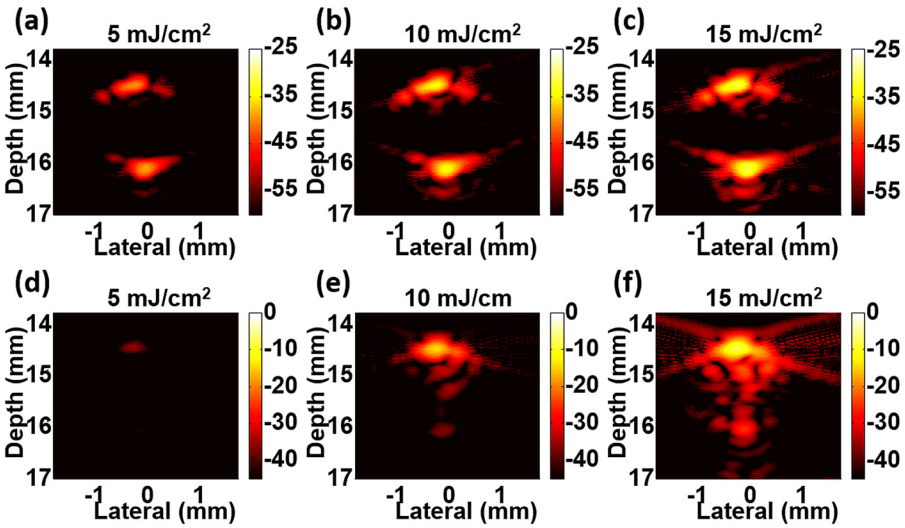

FIG. 2. Photoacoustic images of samples in the tube at different laser fluences: ink solution (a)-(c) and dispersion of nanoemulsion beads with gold nanospheres (d)-(f). Note that images are shown with different dynamic ranges and different levels. Ink: −60 dB to −25 dB. Nanoemulsion beads: −45 dB to 0 dB.

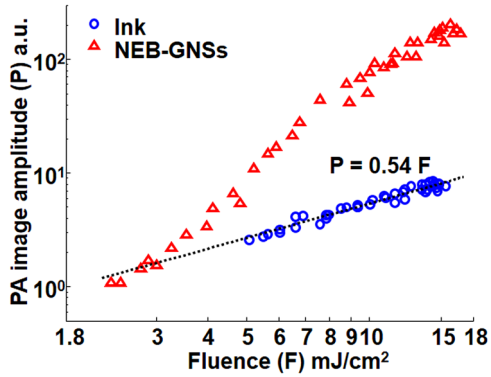

FIG. 3. Photoacoustic image amplitude of ink (blue circle) and NEB-GNSs (red triangle) versus laser fluence.

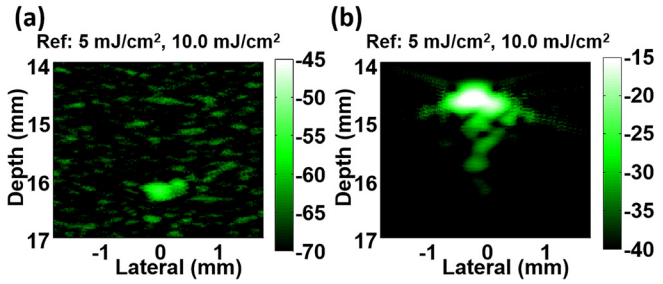

FIG. 4. Differential photoacoustic images of ink (a) and NEB-GNSs (b) at a laser fluence of 10 mJ/cm^2. The reference image is at 5 mJ/cm^2. Images are normalized to the maximum of the original images in Fig. 2 (0 dB) and shown with a dynamic range of 25 dB. Note that images are shown at different levels: −70 dB to −45 dB for ink and −40 dB to −15 dB for NEB-GNSs. The contrast between the two differential images is larger than 40 dB.

larger dynamic range for NEB-GNSs (45 dB versus 35 dB for ink) indicates greater nonlinear signal increase compared to the ink sample over the range of energies used. The maximum display level, 0 dB, is defined as the maximum value in the images of NEB-GNSs.

The PA image amplitude representing the sum of every pixel value within the tube is plotted as a function of laser fluence on a log-log scale in Fig. 3. For ink (blue circles), all data points can tightly fit to a linear equation (dotted line). For NEB-GNSs, this linear relation is only valid under a laser fluence threshold (~3.5 mJ/cm^2), and the amplitude grows non-linearly after the laser fluence exceeds this threshold. At 15 mJ/cm^2, the image amplitude of NEB-GNSs increases by more than 24 times (27.7 dB) that of the ink sample.

To demonstrate that the nonlinear NEB-GNSs can be used to enhance detection specificity in PA molecular imaging, a scale-differential scheme was used. First, a reference image IM_{F0} at laser fluence F_0 was chosen. At every laser fluence F, a linearly scaled image $SIM_{F/F0}$ can be obtained from IM_{F0} according to the ratio of F to F_0

$$SIM_{F/F0} = IM_{F0} \times \frac{F}{F_0}. \quad (1)$$

The differential image $DIM_{F/F0}$ at laser fluence F is obtained by subtracting the scaled reference image from the image IM_F at that laser fluence

$$DIM_{F/F0} = IM_F - SIM_{F/F0}. \quad (2)$$

Fig. 4 presents examples of differential images of the ink sample (Fig. 4(a)) and NEB-GNSs (Fig. 4(b)), both normalized to the maximum (0 dB) of the original image. As expected, the differential image $DIM_{10/5}$ shows nearly complete subtraction for the linear ink sample. The small residue at the bottom of the tube is due to imperfect subtraction and is at the background noise level. In contrast, the differential image of NEB-GNSs, $DIM_{10/5}$, exhibits an enormous residue, with more than 40 dB contrast compared to the differential image of the ink sample. The images are shown with the same dynamic range (25 dB), but at a 30 dB level difference between NEB-GNSs (maximum at −15 dB) and ink (maximum at −45 dB). These results demonstrate the potential of the proposed contrast agent to enhance the specificity of detecting targeted objects in PA molecular imaging by suppressing any background absorber with a linear PA response.

To further investigate the nonlinear behavior of NEB-GNSs, primarily determined by the nonlinear expansion of bubbles, various simple functions, such as parabola, higher order polynomial functions, or exponentials, were used to fit the curve of NEB-GNSs in Fig. 3. Unfortunately, a simple functional form does not capture the behavior of the nonlinear curve. The amplitude obtained by summing all signals within the tube region may not be a valid way to express the behavior of bubble formation and subsequent acoustic generation of a single nanoagent, especially when the phantom is not illuminated homogeneously within the entire tube volume and not all agents are activated at the same time. Also, the characteristics of NEB-GNSs may change at every energy level. Quantification of this nonlinear phenomenon to better understand the relationship between PA amplitude and laser fluence may be feasible using a numerical simulation with a realistic physical model describing this process.

By consecutively sweeping the energy both up and down several times, reproducibility of the non-linearity was demonstrated for NEB-GNSs. However, the amplitude decreases slowly as scan time increases (i.e., degradation toward a linear relation). This is evidence that not all agents are activated at the same time, and they may be slightly degraded on every sweep cycle. This degradation process will be investigated in future studies using a set of NEB-GNSs dispersions of varying concentration irradiated over a range of illumination conditions.

Delivering an ultrasound probe pulse simultaneously, or right after laser-activated bubble generation, enables contrast-enhanced ultrasound imaging as well, in terms of increased backscattered signal and harmonic generation. This agent and technique can be easily implemented in any integrated ultrasound/PA imaging system. With simultaneous laser/ultrasound probing, targeted contrast-enhanced ultrasound imaging and targeted therapy with high intensity focused ultrasound (HIFU) can be envisioned for cardiovascular diagnostic and therapeutic (i.e., theranostic) applications such as blood clot detection and subsequent disruption. However, according to our previous studies,[15,16] the lifetime of the bubbles is about 1–2 μs, which requires precise timing control to deliver the ultrasound pulse before the bubble

collapses. Optimizing the laser irradiation parameters (e.g., pulse duration and laser fluence) and nanoemulsion bead properties (e.g., size and shell material) to create a long-lived bubble is one of our next steps.

In summary, we have proposed a composite contrast agent, NEB-GNSs, to enhance both sensitivity and specificity in PA molecular imaging. When the applied laser fluence exceeds a threshold, the PA signal amplitude of NEB-GNSs is significantly larger (27.7 dB at a laser fluence of 15 mJ/cm^2) than that of a linear agent with the same optical absorption, demonstrating dramatically enhanced sensitivity. By applying a scale-differential scheme on energy-swept PA images, the linear agent was suppressed to the background noise level, while large subtraction residues remain for nonlinear NEB-GNSs, with 40 dB contrast enhancement, demonstrating dramatically enhanced specificity. The fairly low activation laser fluence threshold ($\sim$3.5 mJ/cm^2) implies the use of NEB-GNSs for non-invasive biomedical imaging, since it is possible to achieve such a fluence level at millimeters to a couple of centimeters depth and still within the laser medical safety limits. Furthermore, the temperature of bubble formation of the perfluorohexane core is only 56 °C, and it can be reached in nanoseconds, minimizing heat diffusion to harm surrounding normal cells and thus making this contrast agent safe and applicable for potential *in vivo* applications.

This work was supported in part by NIH RO1EB016034, R01CA170734, T32CA138312, and NSF 0645080, the Life Sciences Discovery Fund 3292512, and the Department of Bioengineering at the University of Washington.

[1]L. V. Wang, *Photoacoustic Imaging and Spectroscopy* (CRC, Boca Raton, FL, 2009).
[2]S. A. Ermilov, T. Khamapirad, A. Conjusteau, M. H. Leonard, R. Lacewell, K. Mehta, T. Miller, and A. A. Oraevsky, J. Biomed. Opt. **14**(2), 024007 (2009).
[3]H. Li and L. V. Wang, Phys. Med. Biol. **54**(19), R59 (2009).
[4]P. C. Li, C. R. C. Wang, D. B. Shieh, C. W. Wei, C. K. Liao, C. Poe, S. Jhan, A. A. Ding, and Y. N. Wu, Opt. Express **16**(23), 18605 (2008).
[5]A. Agarwal, S. W. Huang, M. O'Donnell, K. C. Day, M. Day, N. Kotov, and S. A. Ashkenazi, J. Appl. Phys. **102**(6), 064701 (2007).
[6]A. Zerda, Z. Liu, S. Bodapati, R. Teed, S. Vaithilingam, B. T. Khuri-Yakub, X. Chen, H. Dai, and S. S. Gambhir, Nano Lett. **10**, 2168 (2010).
[7]L. V. Wang and H.-i. Wu, *Biomedical Optics: Principles and Imaging* (Wiley, New York, 2007).
[8]C. Miller, G. V. Doyle, and L. W. M. M. Terstappen, J. Oncol. **2010**, 617421.
[9]K. Larson-Smith and D. C. Pozzo, Langmuir **28**(32), 11725 (2012).
[10]A. Karabutov, N. B. Podymova, and V. S. Letokhov, Appl. Phys. B **63**(6), 545 (1996).
[11]K. Wilson, K. Homan, and S. Emelianov, Nat. Commun. **3**, 618 (2012).
[12]J.-W. Kim, E. I. Galanzha, E. V. Shashkov, H.-M. Moon, and V. P. Zharov, Nat. Nanotechnol. **4**, 688 (2009).
[13]K. Larson-Smith and D. C. Pozzo, Soft Matter **7**(11), 5339 (2011).
[14]G. Frens, Nat. Phys. Sci. **241**(105), 20 (1973).
[15]C.-W. Wei, K. Larson-Smith, I. Pelivanov, C. Perez, J. Xia, D. Pozzo, T. J. Matula, and M. O'Donnell, Proc. SPIE **8581**, 858112 (2013).
[16]C.-W. Wei, M. Lombardo, K. Larson-Smith, I. Pelivanov, C. Perez, J. Xia, D. Pozzo, T. J. Matula, and M. O'Donnell, in *IEEE—UFFC Joint Symposia Prague*, 21–25 July Czech Republic, 2013, IUS1-C3-3.